



# Stability analysis of high power, octave spanning, continuous-wave supercontinuum sources based on cascaded Raman scattering in standard telecom fibers

S. ARUN,<sup>1,2</sup> VISHAL CHOUDHURY,<sup>1</sup> V. BALASWAMY,<sup>1</sup> and V. R. SUPRADEEPA,<sup>1,\*</sup>

<sup>1</sup>Centre for Nano Science and Engineering, Indian Institute of Science, Bangalore, India

<sup>2</sup>aruns@iisc.ac.in

\*supradeepa@iisc.ac.in

**Abstract:** Long term spectral and temporal stability of a recently proposed high power, continuous-wave, supercontinuum source has been characterized. The supercontinuum laser, based on telecom fibers as the nonlinear medium and delivering >35W of CW power over an octave spanning bandwidth (880 to >1900nm), was operated continuously for extended periods of time to investigate its spectral stability. The dependence of stability on various parameters such as the wavelength of pumping and output power was studied by pumping the supercontinuum at 3 different wavelengths and at 3 different output power levels. The RMS value of the difference spectrum (spectral change) was used as the metric for comparison. The spectrum was stable with <1 dB variation over a duration of 60 minutes of continuous operation. This small variation is attributed to heating of the fiber and can be further reduced by properly heat sinking the fiber. When the fiber was cooled down to ambient temperature during power cycling tests, the change in spectrum was ~0.4dB. The supercontinuum output power fluctuations were characterized using a fast photo detector and was measured to be within  $\pm 3\%$  in nanosecond time-scales. The stability measured by these experiments demonstrates the efficacy of the source for a variety of applications.

© 2018 Optical Society of America under the terms of the [OSA Open Access Publishing Agreement](#)

## 1. Introduction

Supercontinuum laser sources with optical fiber as the nonlinear medium have gained immense popularity in the last two decades. The demonstration of Photonic Crystal Fiber (PCF) based supercontinuum by Ranka et al. [1], showed unprecedented bandwidth, spectral flatness and brightness, rendering it useful for a variety of applications like spectroscopy, imaging and instrumentation [2–4]. The wave-guiding capability of optical fiber confines light at high intensities and propagate over long lengths resulting in enhanced optical nonlinearities, which is uncommon in the case of supercontinuum generation processes associated with bulk media. And the specialty fibers like PCF can offer very high optical nonlinearity that can generate ultra-broadband supercontinuum that spans over VIS-NIR range [5]. However majority of the supercontinuum sources demonstrated and available in the market so far, are based on pulsed laser sources as the pump, because it is easier to generate sufficient nonlinearity with high peak power pump pulses [6,7]. This results in low spectral density, which is a limitation for most linear measurements. However, CW supercontinuum sources which are pumped using high power pump laser sources like CW fiber lasers, provide higher power spectral density (PSD) over the bandwidth which is a consequence of its high average power. In addition to this, in CW supercontinuum the availability of output light is not limited by pulse repetition rate (always on) in contrast to the case of pulsed supercontinuum sources, which can be useful in applications where fast time domain measurements are needed.

The major hurdle in developing CW supercontinuum sources was the lack of appropriate high power pump laser sources whose emission profile matches with the zero dispersion wavelength (ZDW) of the medium. But PCF offers the freedom to tailor its dispersion profile and bring the ZDW within the Yb laser emission window. This enabled pumping of PCF directly with high power CW Yb laser sources and CW supercontinuum  $\sim 56\text{W}$  was generated [8]. However, the aspects of loss, cost and difficulty in splicing with conventional silica fiber became bottlenecks and hindered the prospects for power scaling of CW supercontinua in PCF [9].

At the same time, CW supercontinuum sources were also demonstrated using more conventional silica specialty fibers called as Highly Nonlinear Fibers (HNLf) as the nonlinear medium [10]. HNLf's can have a ZDW close to  $1.5\ \mu\text{m}$  while also having enhanced optical nonlinearity than the regular silica fibers [11]. Lack of appropriate pump laser sources was again an issue with the HNLf because the only rare earth doped fiber laser that operates in the ZDW wavelength range near  $1.5\ \mu\text{m}$  is Erbium based laser systems. However it is very difficult to achieve higher output power from these Erbium based laser systems with high brightness (single-moded operation) because of high quantum defects associated with conventional pumping at  $976\text{nm}$  and the parasitic lasing by Ytterbium ions at higher powers in the case of lasers based on ErYb co-doped fibers [12]. Hence HNLf based supercontinuum sources are generally pumped using Raman lasers with Yb laser as the pump source [13,14]. Recently, output power of over  $30\text{W}$  was demonstrated using HNLf based CW supercontinuum sources [15]. Generally, the bandwidth of the supercontinuum in HNLf is decided by the longer wavelength cutoff that happens near  $2\ \mu\text{m}$  due to Silica losses present in the fiber. Four-wave mixing (FWM) that happens between the pump at ZDW and the longer wavelength cut-off decides the shorter wavelength cut-off and thus, the total band width of the supercontinuum [16]. Since the ZDW of the HNLf shifts to longer wavelengths due to increased (negative) waveguide dispersion, the short wavelength cut-off also tends to move towards longer wavelength. This limits the bandwidth in the case of HNLf silica fibers. One straightforward way to enhance the bandwidth is to use a different Silica fiber with a smaller ZDW. We had earlier demonstrated a simple module based on standard telecom fiber which could generate a  $34\text{W}$  CW supercontinuum at an efficiency of  $44\%$ . The total bandwidth of the supercontinuum extends over  $1000\text{nm}$  spanning from  $880\text{nm}$  to  $>1900\text{nm}$  with a PSD of  $>1\text{mW/nm}$  from  $880$  to  $1350\ \text{nm}$  and  $>50\text{mW/nm}$  from  $1350$  to  $1900\text{nm}$  with single mode output [17]. This was enabled by its ZDW near  $1300\text{nm}$ . Since we have used standard silica fiber and telecom components for building the supercontinuum laser, they can be easily fusion spliced using the standard splicing machines with negligible losses, and integrated in an all fiber architecture enabling power scaling. Due to the use of low-cost telecom optical fiber as the nonlinear medium, the overall cost of the laser system also is substantially reduced. In addition, the demonstrated supercontinuum sources were color-blind to the input pump wavelengths originating from the Yb fiber laser and could be pumped using any high power Yb doped fiber laser.

In addition to the output power and bandwidth, the stability and repeatability of spectrum in short and long term operation is very important. The temporal output power stability is also important. In this paper, we rigorously characterize the spectral and temporal stability of the supercontinuum laser as a function of output power, pump wavelength and power cycling, over an extended duration of continuous operation. Our results demonstrate the robustness of this simple architecture and should potentially strengthen the case for its efficacy in a variety of applications.

## 2. Architecture and mechanism behind supercontinuum generation

The mechanism behind CW supercontinuum generation has been understood well with simulations and experiments [18]. It starts with the process of modulation instability (MI) when we pump the nonlinear medium, in this case telecom fiber, at its ZDW. MI leads to

breaking down of CW light into pulses which initiates spectral broadening. Once it breaks down into pulses, a variety of nonlinear effects contribute to supercontinuum generation, like FWM, stimulated Raman scattering (SRS), Raman induced frequency shift (RIFS), Dispersive wave generation etc [19]. One of the major challenges associated with supercontinuum generation using telecom fibers was the lack of high power fiber laser source near its ZDW at 1.3  $\mu\text{m}$ . This issue was overcome by building a high efficiency cascaded Raman laser architecture using the concept of distributed feedback architecture [20–24]. Figure 1 shows the schematic of the supercontinuum generation module. This laser utilizes a high power CW Yb laser as the pump source and performs a series of cascaded Raman Stokes shifts to transfer the pump power from Yb laser band into the ZDW in the anomalous dispersion region of the telecom fiber. In order to achieve efficient cascaded Raman conversion, feedback is essential at all intermediate Stokes wavelengths which will induce preferential forward Raman scattering. Raman conversion based on distributed feedback that can provide grating free, wavelength independent feedback was utilized for this purpose.

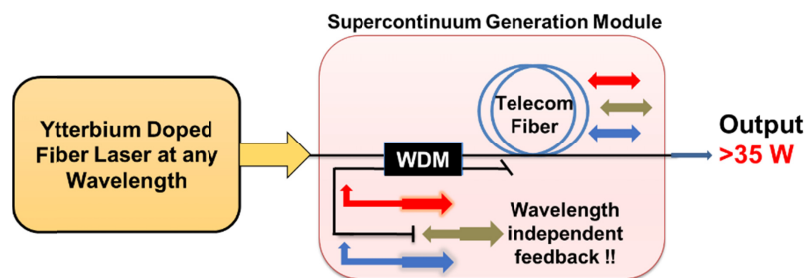


Fig. 1. Architecture of Supercontinuum laser (from [17]) (WDM – Wavelength division multiplexer).

The Yb laser used in this experiment as the pump source is built in a master oscillator power amplifier (MOPA) configuration and is widely tunable from 1064 to 1090nm [25]. The Yb laser emits over 85W of output power across the tuning range. The output from the Yb laser is fed into the telecom fiber through a wavelength division multiplexer (WDM) operating between the 1117/1480nm wavelengths. As the pump power from the Yb fiber laser enters the telecom fiber, it undergoes cascaded stimulated Raman scattering (SRS) and a small amount of Raman shifted components are also scattered in the backward direction. A fraction of this backscattered light is cross coupled into the unused input port of the WDM. A flat cleave is provided in this port. The flat cleave provides a  $\sim 4\%$  Fresnel reflection for the backscattered light which is re-coupled into the telecom fiber. This creates a half-open cavity and preferentially enables forward cascaded Raman conversion. Since all the Raman conversion processes are well seeded, the overall efficiency of the supercontinuum generation was  $\sim 44\%$  with output power of over 35W. Figure 2 shows the octave spanning supercontinuum spectrum when pumped at a wavelength of 1073nm. Previously, with an objective to study the influence of pump wavelength on the supercontinuum spectrum, we had tuned the output wavelength of the Yb laser within this tunable band which in effect enabled us to pump the telecom fiber at different wavelengths near its ZDW. The output spectra remained comparable as the wavelength of pumping was changed [17]. This shows the input wavelength agility of the supercontinuum module and gives us a great degree of freedom in using an Yb laser operating at any wavelength to pump the supercontinuum.

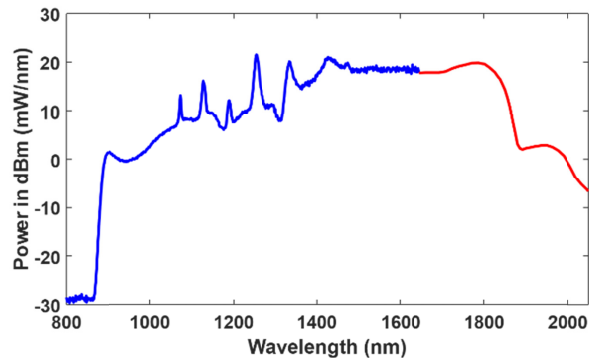


Fig. 2. Supercontinuum spectrum pumped by Yb laser operating at 1073nm (blue part of spectra is captured by OSA and red part of spectra is captured by mid-IR spectrometer).

### 3. Stability of the supercontinuum

The telecom fiber based supercontinuum opens an exciting technique to build compact, low cost, high power, octave spanning CW supercontinuum laser sources. For almost all practical applications it is essential to have a good degree of spectral and temporal stability for the supercontinuum laser source. The stability of the supercontinuum spectrum can potentially vary as a function of the following parameters:

- Pump wavelength – Since the frequency shifts associated with the cascaded Raman conversion are fixed ( $\sim 13.2$  THz per shift in silica fibers), the choice of Yb fiber laser wavelength decides the wavelength of the Raman shifted component which initiates the supercontinuum. It's location with respect to the zero-dispersion wavelength of the fiber can potentially influence the stability of the spectrum.
- Output power – As will be discussed, the output power for a given supercontinuum source demonstrates a saturation behavior with respect to input power. In such a circumstance, it would be essential to characterize the stability as a function of region of operation of output power, whether it is in the growth region or in the saturation region.
- Effect of temperature of the fiber – Owing to high powers of operation, it would be important to characterize any variations in stability of the spectrum due to heating of the fiber.

In this work, we investigate comprehensively, the spectral stability as the parameters discussed above are varied. The stability of the spectrum is characterized through acquiring spectra continuously as a function of time while the source is run for an extended period of time (15mins to 60mins). The RMS value of the difference between the initial and final spectra is used as the metric to evaluate the spectral stability of supercontinuum. For the measurements in this work, we consider a range from 930 to 1700nm, which is within the measurement limits of our optical spectrum analyzer (OSA). We confine the quantitative measurements to the OSA data alone since the instrument is commercial (Yokogawa AQ6370D) and has a specified spectral flatness of  $\sim 0.1$  dB.

#### 3.1 Spectral stability vs. pumping wavelength

In order to evaluate the stability of the spectrum with respect to pumping wavelength, we have operated the Yb laser at three different pump wavelengths at 1070, 1076 and 1082 nm. Corresponding to these pump wavelengths, the Raman shifted component of each near the zero-dispersion wavelength of the fiber is 1318nm, 1327nm and 1337nm. The ZDW of the telecom fiber is tentatively at 1310nm and in all the three cases, the Raman shifted component

is close to and in the anomalous dispersion side of the ZDW as desired. Figure 3(a) shows the output power of the supercontinuum as a function of the input power from the Yb doped fiber laser for the 1070nm case. The output power vs input power is similar for each of the pump wavelengths. The difference spectrum between  $t = 0\text{min}$  and  $t = 15\text{min}$  for the 3 different wavelengths was evaluated at different supercontinuum powers (given in Table 1). The RMS value of the difference spectrum gives a quantitative measure on the spectral change with continuous operation. Figure 3(b), 3(c), 3(d) shows the difference spectrum at a supercontinuum output power of 36.7W (corresponds to 85 W pump power) for different wavelengths of pumping. For all 3 pump wavelengths the RMS value for the difference spectrum is less than 1dB which indicates excellent spectral stability at the different wavelengths of pumping. This indicates that spectral stability is not strongly dependent on the wavelength of pumping. It is important here to note that this measurement is only on the spectral stability and not on the actual spectral shape of the supercontinuum which can vary to a higher degree based on the pump wavelength [17].

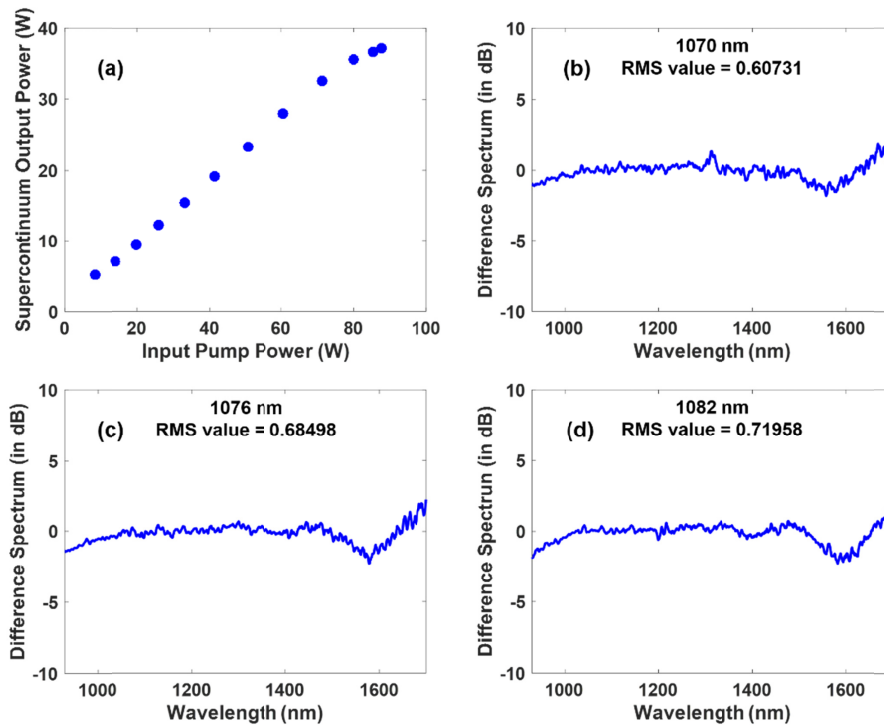


Fig. 3. (a) Supercontinuum output power plot (b), (c), (d) Difference spectrum plots for 1070, 1076, 1082nm pumping.

Table 1. RMS Values of Difference Spectrum for Different Pump Wavelengths and Powers

Pump Wavelength (nm)	Supercontinuum Output Power (W)		
	35.5 W	36.7 W	37.2 W
1070	0.6393	0.6073	0.7879
1076	0.575	0.685	0.9118
1082	0.5418	0.719	1.0808

### 3.2 Spectral stability vs. output power

The output power plot of the supercontinuum is shown in the Fig. 3(a) for the case of 1070nm pumping. The output power starts saturating for an input pump power above 80W onwards

because, with increase in power, due to SRS, the supercontinuum spectrum tends to extend towards longer wavelengths. However the transmission loss in silica fiber increases exponentially ( $>10\text{dB/km}$ ) beyond  $1900\text{nm}$  thereby terminating the spectrum and the excess pump power is lost as heat due to absorptive losses. This limits the maximum output power from the supercontinuum to be  $\sim 37\text{W}$  for a  $2\text{ km}$  long telecom fiber as the nonlinear medium. However, power scaling of the same supercontinuum source can be achieved by using a shorter length of fiber with higher input pump power. Continuous wave supercontinua with output powers as high as  $70\text{W}$  has been demonstrated using the same architecture [26]. Here we characterize the spectral stability for supercontinuum output powers ranging from of  $35\text{--}37\text{ W}$  (corresponding to the transition from the growth to the saturation region) obtained through pump power ranging from  $80$  to  $87\text{W}$ . This was repeated for the three different pump wavelengths as well, and the results are shown in Table 1.

It can be seen that the RMS value for the difference spectrum is  $\sim 1\text{ dB}$  or lower for all cases. However as the output reaches maximum power (saturation) there is an increase in the RMS value of the difference spectra. This is counter-intuitive since it is expected that in the saturation region, owing to less of an impact the variations of input power has on output power, the spectra might be more stable. This seems to indicate the potential role of the temperature parameter in influencing the spectra. Due to higher absorptive losses, it is anticipated that the spool of fiber rises to a higher temperature, closer to saturation.

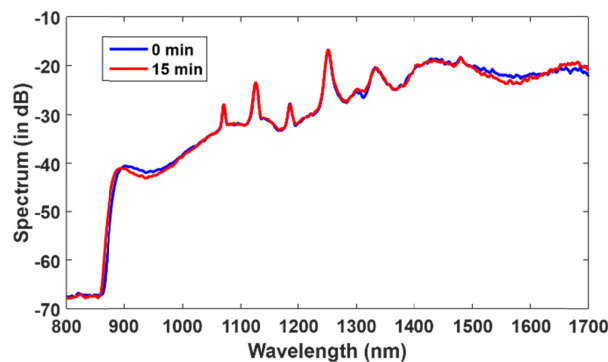


Fig. 4. Supercontinuum spectrum at beginning (blue,  $t = 0$ ), and ending of a continuous run (red,  $t = 15\text{ min}$ ).

Figure 4 shows a representative data for the variation in initial and final spectrum ( $1070\text{ nm}$  pumping at an output power of  $36.7\text{W}$ ). The dip in spectrum that happens near the  $1570\text{ nm}$  and  $930\text{nm}$  occurs gradually with time, along with the rise in temperature of fiber. A rough measurement of increase in temperature of fiber by  $30\text{deg}$  was made using a Fluke Ti-400 thermal camera. This could in principle be higher since the temperature of inner loops of the fiber loops on spool weren't accessible for imaging using the thermal camera. And since the fiber was not heat sinked (wound on a plastic spool), the temperature increased cumulatively over time.

### 3.3 Effect of temperature on the spectral profile

The effect of temperature variation on supercontinuum profile was studied by Martin-Lopez et.al [27], using a CW pump and nonzero dispersion-shifted fiber (NZDF). A change in spectral shape and bandwidth was observed with variation in temperature. It was pointed out that, the optical nonlinear coefficient, which accounts for all the FWM processes, including MI, undergoes a fall in its value with increase in temperature at a rate of  $-0.24\%/^{\circ}\text{C}$  [28]. This reduces the effective gain for FWM and the pump power distribution becomes less uniform across the spectrum, thereby affecting the spectral flatness of the supercontinuum. The

bandwidth of the supercontinuum shows a slight enhancement with rise in temperature, which can be attributed to the reduction in fiber chromatic dispersion [29,30]. The temperature dependence of Raman gain response is expected to be negligible within this range of temperature variation [31]. Since all these are temperature induced variations, the changes in the spectral profile due to their effects can be reverted by cooling down the fiber. To observe this we have pumped the supercontinuum at 1070nm with an output power of 37.2W (max power). And the difference between the spectrum at turn on ( $t = 0$ min) and at the end of cycle ( $t = 45$ min) which includes 15min of continuous operation and then a settling period of 30 min for cooling the fiber to the ambient temperature is shown in Fig. 5.

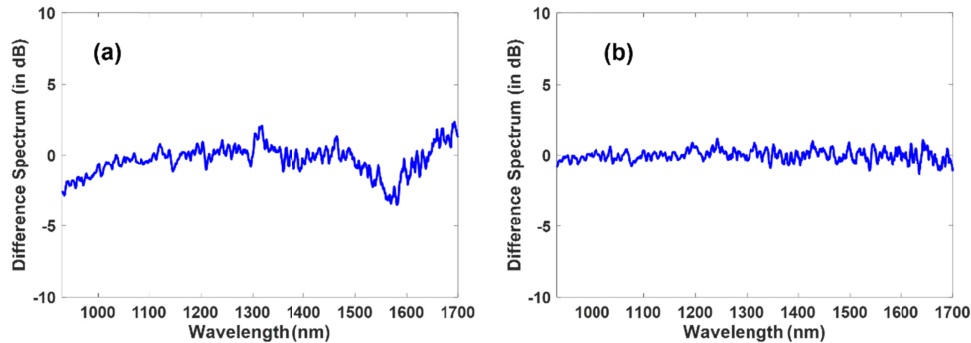


Fig. 5. Difference spectrum during power cycling (a) after 15 min of continuous run (b) after 30 min settling period.

The RMS value for the difference spectrum in Fig. 5(b) is  $\sim 0.39$ dB in contrast to  $\sim 0.79$ dB in Fig. 5(a). This shows that the spectrum has mostly recovered back to its original shape during power cycling. Therefore by taking appropriate measures to heat sink the fiber, the stability of the spectrum can be ensured for extended period of operation. This measurement also demonstrates an important aspect of the source which is useful. The spectra of the supercontinuum source on repeated turn-on (even for time durations of 45minutes and beyond) are very similar. This recovery of the same spectra on repeated turn-ons would be an interesting feature which prevents the need for periodic recalibrating of the source spectra.

In order to validate the relationship between increase in temperature of the fiber and the spectral stability (RMS variations in the difference spectrum), we have operated the supercontinuum laser for one hour continuously at an output power of  $\sim 37$ W. The temperature profile of the fiber spool was measured and monitored continuously using a thermal camera (Ti-400, Fluke) and the supercontinuum spectrum was acquired intermittently over the entire duration of operation. As shown in Fig. 6(a), at a constant power operation of 37W, the temperature first increases rapidly with time and then settles to a temperature of  $\sim 62$  degree Celsius. Correspondingly, there is a substantial change in the spectrum in the initial period. In Fig. 6(b) we have also shown the RMS change for the difference spectrum over a 30 minutes time interval, once the temperature of the spool has settled. The RMS variation of the difference spectrum is  $< 0.4$ dB once the temperature has settled. This clearly indicates that after the warm-up period, the spectral stability is enhanced substantially.

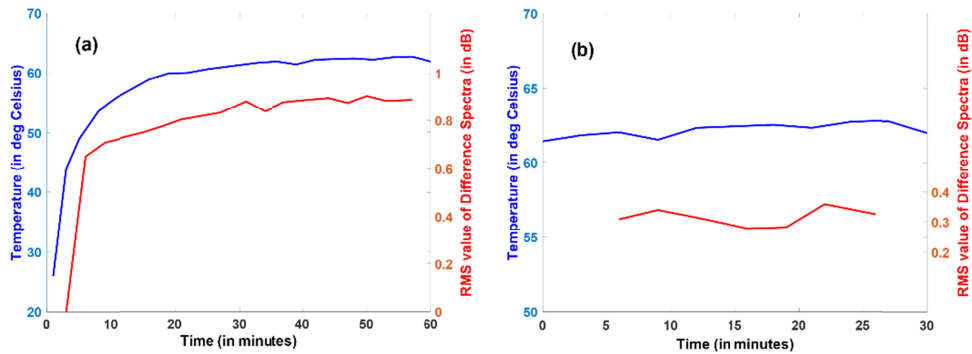


Fig. 6. Change in (a) temperature profile of fiber spool and RMS value of the difference spectrum over time (b) RMS variation of difference spectrum after achieving the steady state fiber temperature.

### 3.4 Temporal stability

Other than the spectral stability of supercontinuum, one important requirement is to have a stable output power with minimal fluctuations. The supercontinuum here is effectively pumped with a Raman fiber laser which is known to have high relative intensity noise (RIN) features at the output [32]. The temporal features in the Raman laser output is expected to be in picosecond timescale which is related to its coherence time and bandwidth [33,34]. It has been shown theoretically and experimentally that a partially coherent CW pump source can facilitate MI process better than a coherent CW pump source, which therefore enhances the supercontinuum growth [35,36]. And the output of the supercontinuum involves time average of solitons of different frequencies appearing at random durations [33].

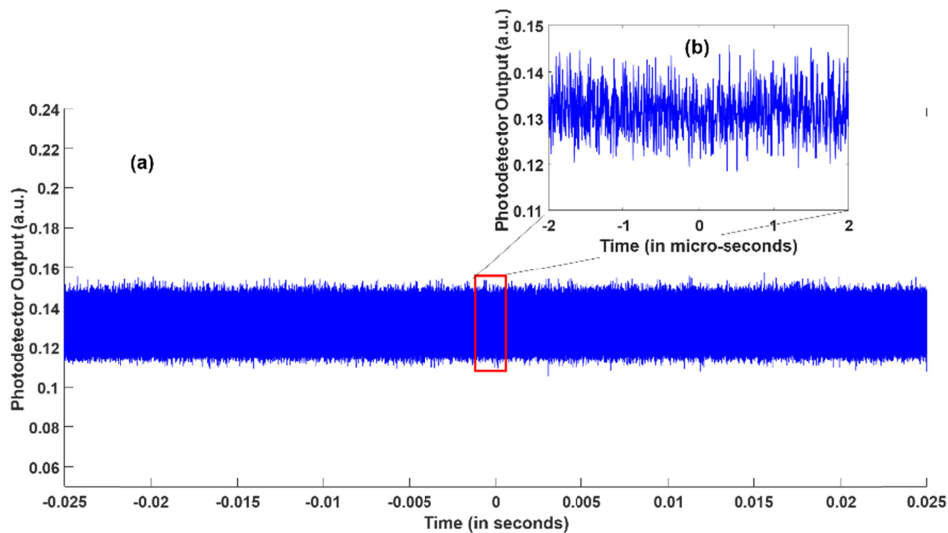


Fig. 7. (a) Time domain fluctuations at the output of supercontinuum (b) inset shows the fluctuations at a faster time scale.

As far as the output power stability of a CW supercontinuum is concerned, we are interested in the temporal features or fluctuations that are in the microsecond time scales and slower. This is based on potential timescales of measurements utilizing the supercontinuum source. To measure this we used a 150MHz Thorlabs PDA10CF-EC photodetector and the rms deviation of the output power fluctuation measured using the fast photodetector is  $\sim \pm$



3%, when measured over several seconds of acquisition, using Keysight DSO 9104A Infiniium digital storage oscilloscope with an acquisition rate of 2 billion samples per second. The output of photodetector at different time scales (along with a zoomed in image) is shown in Fig. 7. This indicates that for even relatively fast measurement in the microsecond time-scales, the supercontinuum source is temporally stable with no extreme or noisy events observed. This temporal behavior was found to be similar for all pump wavelengths at the three different power levels investigated.

#### 4. Conclusion

We have investigated the spectral and temporal stability of the supercontinuum for extended period of operation (~60min) and also studied the dependence of pumping wavelength and output power on the supercontinuum stability. It was observed that the supercontinuum spectrum was very stable (~1 dB or lower RMS value for spectral change) for different pumping wavelengths, over the entire duration of operation. This highlights the robustness of the telecom fiber based supercontinuum, in terms of using an Yb fiber laser operating at any wavelength to pump the supercontinuum without compromising on the stability. The small variation in the spectral profile with time was attributed to the heating of fiber. However, the spectral profile reverted back to its original shape when the fiber was allowed to cool down to the ambient temperature. Therefore by appropriate heat sinking of the optical fiber, spectral stability can be improved much better over extended duration of operation. In addition, we demonstrated that, even without the heat-sinking, after a warm-up period, the supercontinuum spectra becomes very stable over extended durations of operation. The standard deviation for fluctuation in output power with time was also measured using a fast photodetector. The standard deviation was measured to be  $\sim \pm 3\%$ , when measured over several seconds of acquisition, measured with a 150MHz photodetector. With these measurements the SMF based CW supercontinuum has demonstrated excellent long term spectral and temporal stability and reliability.

#### Funding

SERB, Govt of India (SB/S3/EECE/0149/2015).

#### References

1. J. K. Ranka, R. S. Windeler, and A. J. Stentz, "Visible continuum generation in air-silica microstructure optical fibers with anomalous dispersion at 800 nm," *Opt. Lett.* **25**(1), 25–27 (2000).
2. D. M. Owen, E. Auksoorius, H. B. Manning, C. B. Talbot, P. A. A. de Beule, C. Dunsby, M. A. A. Neil, and P. M. W. French, "Excitation-resolved hyperspectral fluorescence lifetime imaging using a UV-extended supercontinuum source," *Opt. Lett.* **32**(23), 3408–3410 (2007).
3. P.-L. Hsiung, Y. Chen, T. Ko, J. Fujimoto, C. de Matos, S. Popov, J. Taylor, and V. Gapontsev, "Optical coherence tomography using a continuous-wave, high-power, Raman continuum light source," *Opt. Express* **12**(22), 5287–5295 (2004).
4. T. Morioka, H. Takara, S. Kawanishi, O. Kamatani, K. Takiguchi, K. Uchiyama, M. Saruwatari, H. Takahashi, M. Yamada, T. Kanamori, and H. Ono, "1Tbit/s (100 Gbit/sx10 channel) OTDM/WDM transmission using a single supercontinuum WDM source," *Electron. Lett.* **32**(10), 906–907 (1996).
5. J. C. Travers, A. B. Rulkov, B. A. Cumberland, S. V. Popov, and J. R. Taylor, "Visible supercontinuum generation in photonic crystal fibers with a 400 W continuous wave fiber laser," *Opt. Express* **16**(19), 14435–14447 (2008).
6. S. Coen, A. H. Chau, R. Leonhardt, J. D. Harvey, J. C. Knight, W. J. Wadsworth, and P. St. J. Russell, "White-light supercontinuum generation with 60-ps pump pulses in a photonic crystal fiber," *Opt. Lett.* **26**(17), 1356–1358 (2001).
7. G. Genty, M. Lehtonen, H. Ludvigsen, J. Broeng, and M. Kaivola, "Spectral broadening of femtosecond pulses into continuum radiation in microstructured fibers," *Opt. Express* **10**(20), 1083–1098 (2002).
8. A. Jin, H. Zhou, X. Zhou, J. Hou, and Z. Jiang, "High-power ultraflat near-infrared supercontinuum generation pumped by a continuous amplified spontaneous emission source," *IEEE Photonics J.* **7**(2), 1–9 (2015).
9. M. Takahashi, R. Sugizaki, J. Hiroishi, M. Tadakuma, Y. Taniguchi, and T. Yagi, "Low-Loss and Low-Dispersion-Slope Highly Nonlinear Fibers," *J. Lightwave Technol.* **23**(11), 3615–3624 (2005).

10. J. W. Nicholson, A. K. Abeeluck, C. Headley, M. F. Yan, and C. G. Jørgensen, "Pulsed and continuous-wave supercontinuum generation in highly nonlinear, dispersion-shifted fibers," *Appl. Phys. B* **77**(2-3), 211–218 (2003).
11. M. Onishi, T. Okuno, T. Kashiwada, S. Ishikawa, N. Akasaka, and M. Nishimura, "Highly nonlinear dispersion shifted fibers and their application to broadband wavelength converter," *Opt. Fiber Technol. Mater. Devices Syst.* **4**(2), 204–214 (1998).
12. G. Sobon, P. Kaczmarek, A. Antonczak, J. Sotor, and K. M. Abramski, "Controlling the 1  $\mu\text{m}$  spontaneous emission in Er/Yb co-doped fiber amplifiers," *Opt. Express* **19**(20), 19104–19113 (2011).
13. A. K. Abeeluck and C. Headley, "Continuous-wave pumping in the anomalous- and normal-dispersion regimes of nonlinear fibers for supercontinuum generation," *Opt. Lett.* **30**(1), 61–63 (2005).
14. B. H. Chapman, S. V. Popov, and R. Taylor, "Continuous wave supercontinuum generation through pumping in the normal dispersion region for spectral flatness," *IEEE Photonics Technol. Lett.* **24**(15), 1325–1327 (2012).
15. V. Choudhury, S. Arun, R. Prakash, and V. R. Supradeepa, "High-power continuous-wave supercontinuum generation in highly nonlinear fibers pumped with high-order cascaded Raman fiber amplifiers," *Appl. Opt.* **57**(21), 5978–5982 (2018).
16. A. K. Abeeluck, C. Headley, and C. G. Jørgensen, "High-power supercontinuum generation in highly nonlinear, dispersion-shifted fibers by use of a continuous-wave Raman fiber laser," *Opt. Lett.* **29**(18), 2163–2165 (2004).
17. S. Arun, V. Choudhury, V. Balaswamy, R. Prakash, and V. R. Supradeepa, "High power, high efficiency, continuous-wave supercontinuum generation using standard telecom fibers," *Opt. Express* **26**(7), 7979–7984 (2018).
18. G. P. Agrawal, *Nonlinear Fiber Optics* (Academic, 2007).
19. J. M. Dudley, G. Genty, and S. Coen, "Supercontinuum generation in photonic crystal fiber," *Rev. Mod. Phys.* **78**(4), 1135–1184 (2006).
20. S. A. Babin, I. D. Vatnik, A. Yu. Laptev, M. M. Bubnov, and E. M. Dianov, "High-efficiency cascaded Raman fiber laser with random distributed feedback," *Opt. Express* **22**(21), 24929–24934 (2014).
21. L. Zhang, H. Jiang, X. Yang, W. Pan, and Y. Feng, "Ultra-wide wavelength tuning of a cascaded Raman random fiber laser," *Opt. Lett.* **41**(2), 215–218 (2016).
22. S. Arun, V. Balaswamy, S. Aparanji, and V. R. Supradeepa, "High power, grating-free, cascaded Raman fiber lasers," 2017 Conference on Lasers and Electro-Optics Europe & European Quantum Electronics Conference (CLEO/Europe-EQEC), 2017, pp. 1–1.
23. V. Balaswamy, S. Arun, S. Aparanji, V. Choudhury, and V. R. Supradeepa, "High-power, fixed, and tunable wavelength, grating-free cascaded Raman fiber lasers," *Opt. Lett.* **43**(7), 1574–1577 (2018).
24. V. R. Supradeepa, Y. Feng, and J. W. Nicholson, "Raman fiber lasers," *J. Opt.* **19**(2), 023001 (2017).
25. V. Balaswamy, S. Aparanji, G. Chayran, and V. R. Supradeepa, "Tunable wavelength, tunable linewidth, high power ytterbium doped fiber laser," in *13th International Conference on Fiber Optics and Photonics, OSA Technical Digest* (online) (Optical Society of America 2016), paper Tu3E.4. (2016).
26. S. Arun, V. Choudhury, V. Balaswamy, and V. R. Supradeepa, "Power Combined, Octave-spanning, CW Supercontinuum using Standard Telecom Fiber with Output Power of 70W," in Conference on Lasers and Electro-Optics, OSA Technical Digest (Optical Society of America, 2018), paper SM1K.5.
27. S. Martin-Lopez, M. Gonzalez-Herraez, P. Corredera, M. L. Hernanz, A. Carrasco, and J. A. Mendez, "Temperature effects on supercontinuum generation using a continuous-wave Raman fiber laser," *Opt. Commun.* **267**(1), 193–196 (2006).
28. Y. Imai and K. Mizuta, "Measurements of thermal effects on four-photon mixing conversion efficiency in an optical fiber," *Opt. Lett.* **25**(19), 1412–1414 (2000).
29. T. Kato, Y. Koyano, and M. Nishimura, "Temperature dependence of chromatic dispersion in various types of optical fiber," *Opt. Lett.* **25**(16), 1156–1158 (2000).
30. G. Ghosh, M. Endo, and T. Iwasaki, "Temperature-dependent Sellmeier coefficients and chromatic dispersions for some optical fiber glasses," *J. Lightwave Technol.* **12**(8), 1338–1342 (1994).
31. S. A. E. Lewis, S. V. Chernikov, and J. R. Taylor, "Temperature-dependent gain and noise in fiber Raman amplifiers," *Opt. Lett.* **24**(24), 1823–1825 (1999).
32. A. K. Abeeluck and C. Headley, "Supercontinuum growth in a highly nonlinear fiber with a low coherence semiconductor laser diode," *Appl. Phys. Lett.* **85**(21), 4863–4865 (2004).
33. F. Vanholsbeeck, S. Martin-Lopez, M. González-Herráez, and S. Coen, "The role of pump incoherence in continuous-wave supercontinuum generation," *Opt. Express* **13**(17), 6615–6625 (2005).
34. A. Mussot, E. Lantz, H. Maillotte, T. Sylvestre, C. Finot, and S. Pitois, "Spectral broadening of a partially coherent CW laser beam in single-mode optical fibers," *Opt. Express* **12**(13), 2838–2843 (2004).
35. D. Anderson, L. Helczynski-Wolf, M. Lisak, and V. Semenov, "Features of modulational instability of partially coherent light: Importance of the incoherence spectrum," *Phys. Rev. E Stat. Nonlin. Soft Matter Phys.* **69**(2), 025601 (2004).
36. R. Prakash V. Choudhury, S. Arun, and V. R. Supradeepa, "Low power generation of equalized broadband CW supercontinua using a novel technique incorporating modulation instability of line broadened pump," *Proc. SPIE* **10528**, 1052817 (2018).